PNAS RESEARCH ARTICLE | NEUROSCIENCE OPEN ACCESS

Two distinct evolutionary conserved neural degeneration pathways characterized in a colonial chordate

Chiara Anselmi[a,b,1], Mark Kowarsky[c], Fabio Gasparini[d], Federico Caicci[d], Katherine J. Ishizuka[a], Karla J. Palmeri[a], Tal Raveh[b], Rahul Sinha[b], Norma Neff[e], Stephen R. Quake[e,f], Irving L. Weissman[b,e,g,1], Ayelet Voskoboynik[a,b,e,g,1,2], and Lucia Manni[d,1,2]

Contributed by Irving L. Weissman; received February 26, 2022; accepted April 21, 2022; reviewed by David H. Rowitch and Irene Salinas

Colonial tunicates are marine organisms that possess multiple brains simultaneously during their colonial phase. While the cyclical processes of neurogenesis and neurodegeneration characterizing their life cycle have been documented previously, the cellular and molecular changes associated with such processes and their relationship with variation in brain morphology and individual (zooid) behavior throughout adult life remains unknown. Here, we introduce *Botryllus schlosseri* as an invertebrate model for neurogenesis, neural degeneration, and evolutionary neuroscience. Our analysis reveals that during the weekly colony budding (i.e., asexual reproduction), prior to programmed cell death and removal by phagocytes, decreases in the number of neurons in the adult brain are associated with reduced behavioral response and significant change in the expression of 73 mammalian homologous genes associated with neurodegenerative disease. Similarly, when comparing young colonies (1 to 2 y of age) to those reared in a laboratory for ∼20 y, we found that older colonies contained significantly fewer neurons and exhibited reduced behavioral response alongside changes in the expression of 148 such genes (35 of which were differentially expressed across both timescales). The existence of two distinct yet apparently related neurodegenerative pathways represents a novel platform to study the gene products governing the relationship between aging, neural regeneration and degeneration, and loss of nervous system function. Indeed, as a member of an evolutionary clade considered to be a sister group of vertebrates, this organism may be a fundamental resource in understanding how evolution has shaped these processes across phylogeny and obtaining mechanistic insight.

colonial chordate | neurodegeneration | regeneration | aging | neural stem cells

Significance

Loss of the brain's functional ability is a common symptom of aging across diverse phyla. While the genetic and molecular mechanisms underlying mammalian neurodegeneration have been studied in depth, very little is known about the evolutionary origin of these traits and their involvement in loss of nervous system function in aged-invertebrate species. Here, we present *Botryllus schlosseri*, a marine colonial tunicate, as a model system for evolutionary neuroscience and the study of neurogenesis, neurodegeneration, and aging. The organism's unique life cycle, as characterized by two distinct yet connected neurodegenerative pathways, offers a novel platform for comparative studies designed to identify the cellular and molecular mechanisms regulating such processes across phylogeny.

Botryllus schlosseri, a marine colonial chordate, has produced valuable insight in the study of tissue regeneration (1, 2), allorecognition (3–6), and stem cells (7, 8). *B. schlosseri* can be developed as a chordate following sexual reproduction, which gives rise to a tadpole that hatches and finds a subtidal surface to attach to, before metamorphosis into a sessile invertebrate. The metamorphosed individual develops 1 to 3 buds (covered by a common gelatinous tunic) that develop the invertebrate body plan, and several individuals anastomose extracorporeal blood vessels in the tunic to form a colony. Every week this colonial organism undergoes a de novo robust regeneration mediated by adult stem cells that participate in the formation of all body organs, including the central nervous system. The lifespan of *B. schlosseri* is plastic and amenable to change. Wild colonies are characterized by short lifespans ranging from several months to a few years (9–12) whereas colonies grown in the laboratory can reach 20 y of age (12–17). Systemic changes occur over time in older colonies, including a slower heartbeat, reduced zooid size, decreased regenerative capacity, a shift in cellular composition (e.g., higher level of engulfing phagocytic, cytotoxic, and pigment cells), and shifting patterns of cyclic gene expression associated with aging (17). Despite the key evolutionary position of *B. schlosseri* as a member of a clade considered to be the sister group of vertebrates (the body plan of the sexually reproduced larval tadpole is along the architecture of most chordate fetuses) (18), and previous literature describing its central nervous system (19–22), little is known about changes in brain morphology, colony behavior, and gene expression associated with the regular, cyclical processes of neural generation and degeneration and how they vary with colony age.

Here we introduce *B. schlosseri* as a model for evolutionary neuroscience. The *B. schlosseri* genome has been sequenced (5) and an atlas of the molecular and morphological signatures of each developmental stage has been previously generated using microscopy and RNA sequencing (RNA-seq) (22). *B. schlosseri* can reproduce either sexually through embryogenesis or asexually through blastogenesis. The sexually produced larvae develop two brains (a functional larval brain and the rudiment of the adult brain), a sensory organ detecting light and gravity, a notochord, and a dorsal nerve cord. The larval brain (along with the notochord, segmented musculature, and tail) is absorbed during the settlement and metamorphosis

Author contributions: C.A., L.M., A.V., and I.L.W. provided conception and design; C.A., F.G., K.J.I., and K.J.P. provided mariculture, observation and sample collection; C.A., L.M., F.C., and F.G. provided TEM and confocal, light microscopy; L.M. and F.C. provided 3D reconstructions; C.A, L.M, and F.G. provided behaviour assay; K.J.I. performed brain extraction; K.J.P. and A.V. provided RNA isolation and library preparation; N.F.N. and S.R.Q. provided sequencing; C.A. and M.K. provided transcriptome analysis; F.G., C.A., and M.K. provided statistical analysis; C.A., A.V., L.M., and M.K. wrote the manuscript; and R.S., T.R., and I.L.W. provided technical support and conceptual advice.

Reviewers: D.H.R., University of Cambridge; and I.S., The University of New Mexico.

The authors declare no competing interest.

[1]To whom correspondence may be addressed. Email: irv@stanford.edu, chiara90@stanford.edu, ayeletv@stanford.edu, or lucia.manni@unipd.it.

[2]A.V. and L.M. contributed equally to this work.

This article contains supporting information online at http://www.pnas.org/lookup/suppl/doi:10.1073/pnas.2203032119/-/DCSupplemental.

Published July 11, 2022.

which precedes colony formation. As a sedentary organism, *B. schlosseri* buds new individuals that together live as a colony composed of individual zooids. Each zooid reproduces asexually in weekly, stem cell-mediated budding cycles (7). Budding occurs during this cycle when, simultaneously throughout the colony, a new generation of buds begin to develop into adult individuals. During budding, all organs including the brain, are created anew without passing through a larval (embryonic and fetal) stage. The life of adult zooids lasts ~1 wk after which their bodies undergo a synchronized wave of programmed cell death and phagocytic removal called takeover (i.e., TO) (16, 23) in which the nervous systems of old zooids degenerate in tangent to brain formation in the young buds.

In this study, we describe 2 different pathways of neurodegeneration that occur during the life cycle of the colonial chordate *B. schlosseri*. The first occurs every week as a part of a regenerative developmental cycle that occurs independent of age; the second is associated with colony aging. We integrate neural imaging (transmission electron microscopy [TEM] and confocal), three-dimensional (3D) reconstructions, behavioral assay, and RNA-seq of enriched brains (Fig. 1) to study morphological and molecular changes in brains of adult *B. schlosseri* across developmental stages and ages as associated with changes in zooid behavior. In providing evidence of the cellular and molecular linkages between each neurodegenerative process, we document an unanticipated degree of similarity between the 2 that may be useful in identifying the evolutionary basis of the pathological mechanisms responsible for age-induced loss of neuron structure and function in other phylogeny. Indeed, we argue that given 1) a unique and assayable life cycle, 2) real-time monitoring enabled by transparent body and vasculature, 3) adult tissue specific stem cells that can be enriched and transplanted, 4) morphological differences associated with colony age, and 5) a previously sequenced genome; *B. schlosseri* provides a novel and valuable platform for the study of neurogenesis, neurodegeneration, and evolutionary neuroscience.

Results

The neural complex of *B. schlosseri*, located between the incurrent (oral) and excurrent (atrial) siphons, is composed of a brain (central nervous system [CNS]) and a neural gland complex with the following components: ciliated funnel, dorsal tubercle, neural gland body, and a dorsal organ (Fig. 2 *A–D*). The zooid brain controls siphons, body muscle contractions, and the ciliated cells of the branchial stigmata involved in respiration and food collection. Motor neurons located in the brain send their axons to the effector systems, i.e., muscle cells in the zooid body wall and heart, and ciliated cells (mechanoreceptors) in the oral siphon, branchial sac and gut (20, 21, 24–27). During the weekly cycle of development and degeneration, new brains develop in each growing bud as the brains of older adult zooids degenerate (19, 22).

The Number of Neurons and Immune Cells in the *B. schlosseri* Brain Fluctuates Every Week. To characterize the cellular dynamics of the adult zooid brains during their short-term lifespan (1 wk) we counted the number of neurons that were stained with anti-alpha tubulin antibody (28) and a nuclear marker (DAPI) in the brains each day (Fig. 3*A* and *SI Appendix, Supplementary Data 1*). In early cycle, this number ranged between 750 and 850 (days 1 to 3), reaching its maximum (~900 cells), on day 4 (midcycle). Thereafter the number of neurons decreased (days 5 to 6) until full brain reabsorption at the end of the takeover (day 7) (Figs. 2*E* and 3*B*). These analyses revealed that brains continue to develop in individual adult zooids up to half their individual lifespan, following their maturation in the buds and thereafter undergo neurodegeneration. 3D reconstructions of the zooid neural complex at days 1, 3, 5, and 7 from 1 μm thick histological serial sections confirmed this pattern and also revealed that in early cycle the brain is contiguous with both the neural gland and the dorsal organ and other cells with undifferentiated morphology (i.e., large nuclear/cytoplasmic ratio, absence of vesicles or granules in cytoplasm) (Fig. 2 *J–M* and *SI Appendix*, Fig. S1) that also resemble pioneer nerve cells associated with brain formation in buds (19). In the late cycle, the neural gland and dorsal organ disconnect from the brain and the putative delaminating pioneer cells are not detected.

TEM of zooid brains during days 1, 3, 5, and 7 further revealed that during the early stages (Fig. 2 *F–I*), the brain is composed of a well-organized medulla of packed neurites and

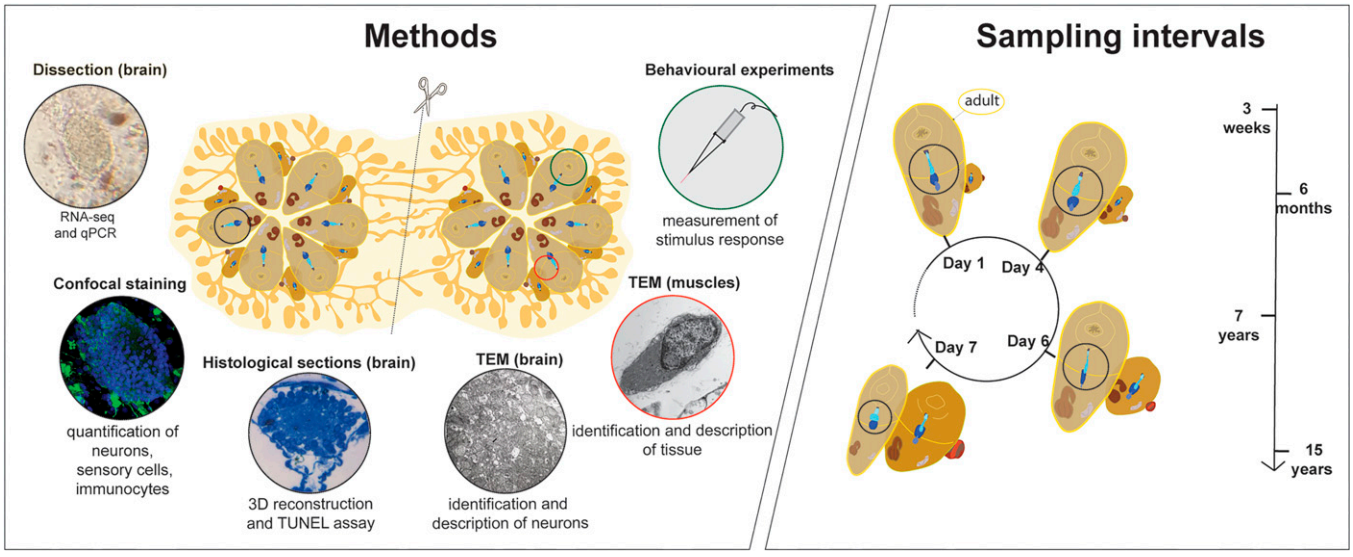

Fig. 1. Sampling and methods used to characterize weekly cycles of neurodegeneration in *B. schlosseri* colonies. Schematic depicting the various methods employed over the course of the investigation including neural complex dissection, confocal staining, histology, TEM, behavioral experiments and the intervals over which neural complex sampling was conducted (over the weekly cycle and with age in adult individuals). Genetically identical subclones prepared via incision and separation were used in diverse experimental groups.

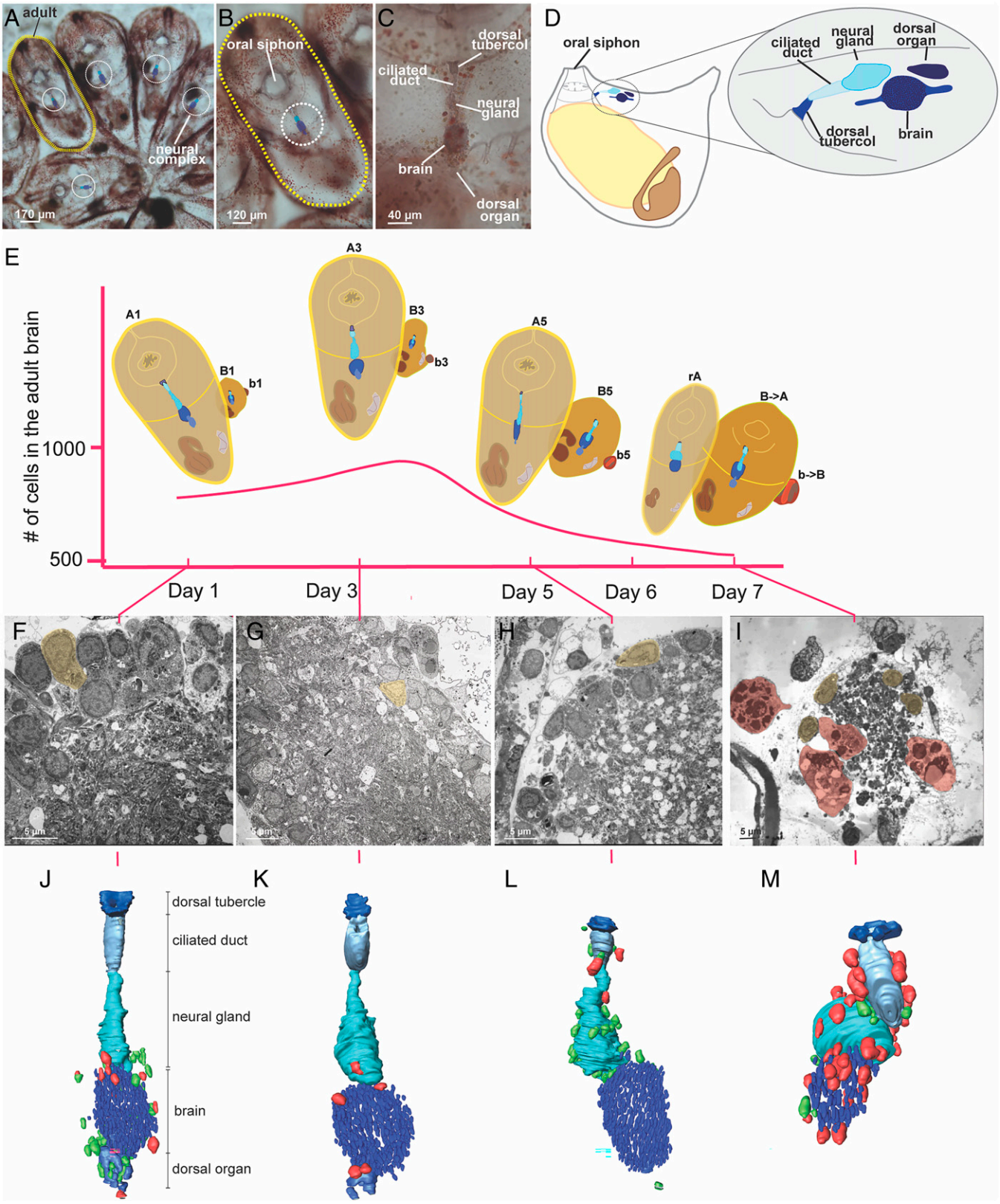

Fig. 2. Every week brains undergo dynamic changes leading to their degeneration that involve immunocytes. *(A–C)* A whole-mount colony (*A*) is formed of several blastozooids, i.e., zooids derived from budding, that are grouped in star-shaped systems; each colony is embedded in the common tunic, the extracellular matrix characteristic of tunicates, where a colonial circulatory system spreads. The latter is composed of blood vessels, joining and functionally coordinating zooids, and terminal ampullae. Each zooid (*B*) has its own neural complex (*C*) located between the oral and atrial siphon and it is formed by 1) a brain (cerebral ganglion), 2) a neural gland, dorsal to the brain that opens into a branchial chamber through a ciliated duct and a dorsal tubercle and 3) a dorsal organ posterior to the gland and dorsal to the brain. *(D)* Illustration of an adult individual in lateral view with an enlarged view of the neural complex. *(E)* Changes in brain neuron number during the weekly cycle. The illustrations highlight the neural complex and its development in the primary bud (B), secondary bud (b), adult (A) and regressing adult (rA). *(F–I)* TEM of a brain respectively at day 1, 3, 5, 7; neurons are highlighted in yellow, phagocytes in red. *(J–M)* 3D reconstructions of the neural complex of an adult at day 1, 3, 5, 7 surrounded by morula (green) and phagocytes (red).

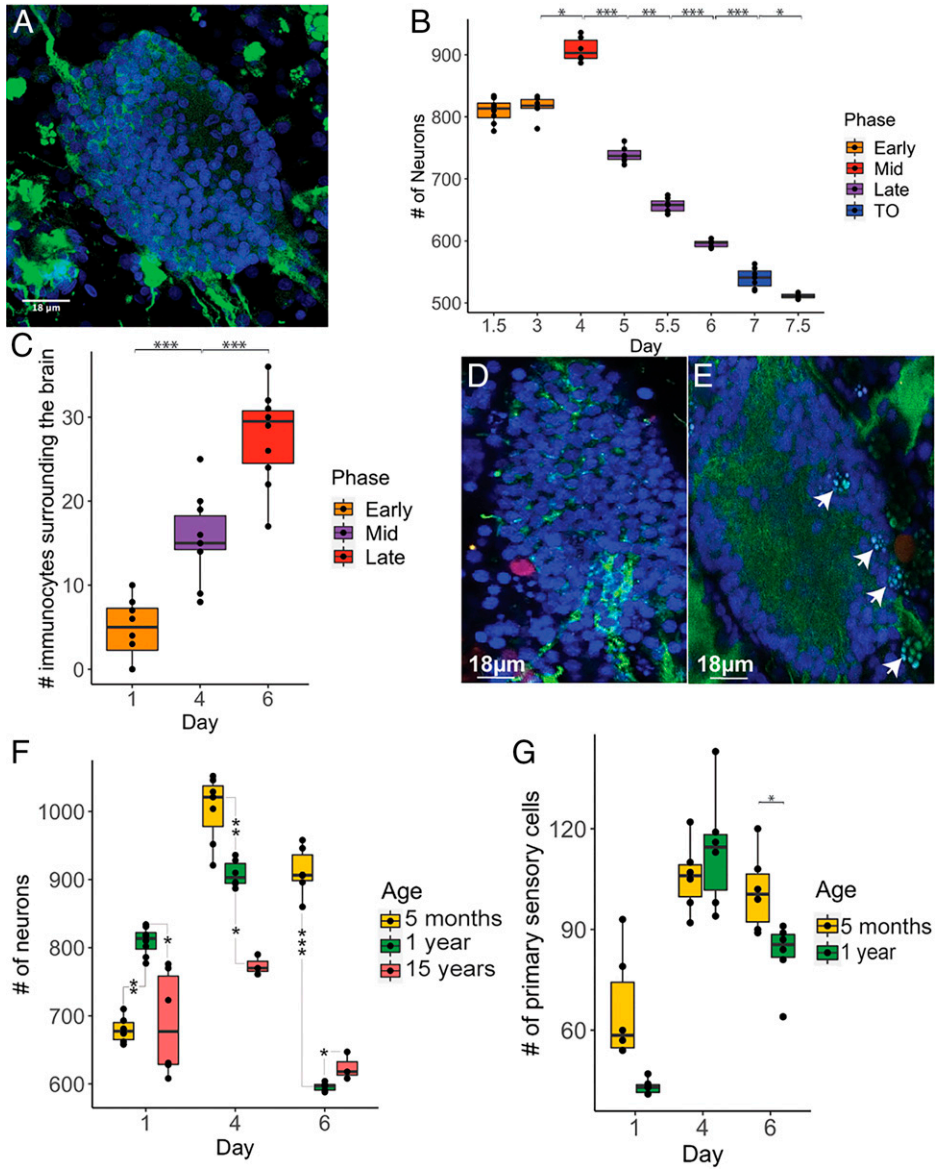

Fig. 3. A progressive decrease in the number of neurons in brains is observed during both the weekly cycle and with age. *(A)* Brain of *B. schlosseri* labeled with anti-alpha tubulin (green) and DAPI (blue). *(B)* Neuron number in adult brains during the weekly cycle; day 1.5 ($n = 8$), day 3 ($n = 6$), day 4 ($n = 6$), day 5 ($n = 6$), day 5.5 ($n = 7$), day 6 ($n = 5$), day 7 ($n = 7$), day 7.5 ($n = 3$). *(C)* Number of immunocytes during the weekly cycle; day 1 ($n = 8$), day 4 ($n = 10$), day 6 ($n = 10$). *(D)* Phagocyte (red) labeled with anti rhamnose–binding lectine (RBL), blue: brain neuron nuclei. *(E)* Morula cells (arrows) in the brain. *(F)* Neuron number during the weekly cycle in adults belonging to 5 mo-, 1 y- and ~15 y- old colonies. *(G)* Sensory cell number during the weekly cycle in 5 mo- and 1 y-old colonies. ANOVA and post hoc test. *P* value < 0.05 (*); *P* value < 0.01 (**); *P* value < 0.001 (***).

an external cortex made of two or three layers of neuronal somata (Fig. 2 *F* and *G*). As the colony approaches takeover, the neurons are arranged in an apparently irregular manner; polymorphic nuclei with condensed chromatin are detected (Fig. 2 *H* and *I* and *SI Appendix*, Fig. S2 and *Supplementary Data 2*). TUNEL assay showed that apoptosis is involved in neurodegeneration (days 5 and 6) (*SI Appendix*, Fig. S3 and *Supplementary Data 3*). Muscle cells proximal to the brain did not degenerate at days 5 and 6, indicating that initial degeneration of the brain precedes the global tissue degeneration observed during takeover (*SI Appendix*, Fig. S4).

During takeover high numbers of circulating immunocytes, including phagocytes and morula cells, are observed. Both cell types are involved in self and nonself recognition and target cell clearance, but while phagocytes engulf target cells, morula cells use cytotoxicity and are also associated with killing allogeneic cells (23, 29–31). Our 3D models and confocal analysis revealed that the number of phagocytes and morula cells in proximity to or within the zooid's neural complex changes over the weekly cycle, reaching a maximum number on day 6 (late cycle toward takeover) (Figs. 2 *J–M* and 3 *C–E* and *SI Appendix*, Fig. S5 and *Supplementary Data 4–6*). While in early-cycle stages (days 1 to 4) the immunocytes are concentrated around and within the brain and the dorsal organ, during late stages they border the neural gland. Both intact and degranulated morula cells were found in close proximity to the brains during this phase (*SI Appendix*, Fig. S6 *B* and *C*) and neuron debris was observed in the vacuoles of phagocytes that invaded the brains (Fig. 2*I* and *SI Appendix*, Fig. S6). The close proximity of neurons and immunocytes and the significant changes in their locations and numbers over the weekly cycle suggest that immunocytes play an important role in neuron protection (morula cells) and removal (phagocytes).

Decrease in Neuron Number Correlates with a Reduced Response to Stimuli. To better understand neurodegeneration in *B. schlosseri* we compared the number of neurons in brains of 5-mo, 1 y- and

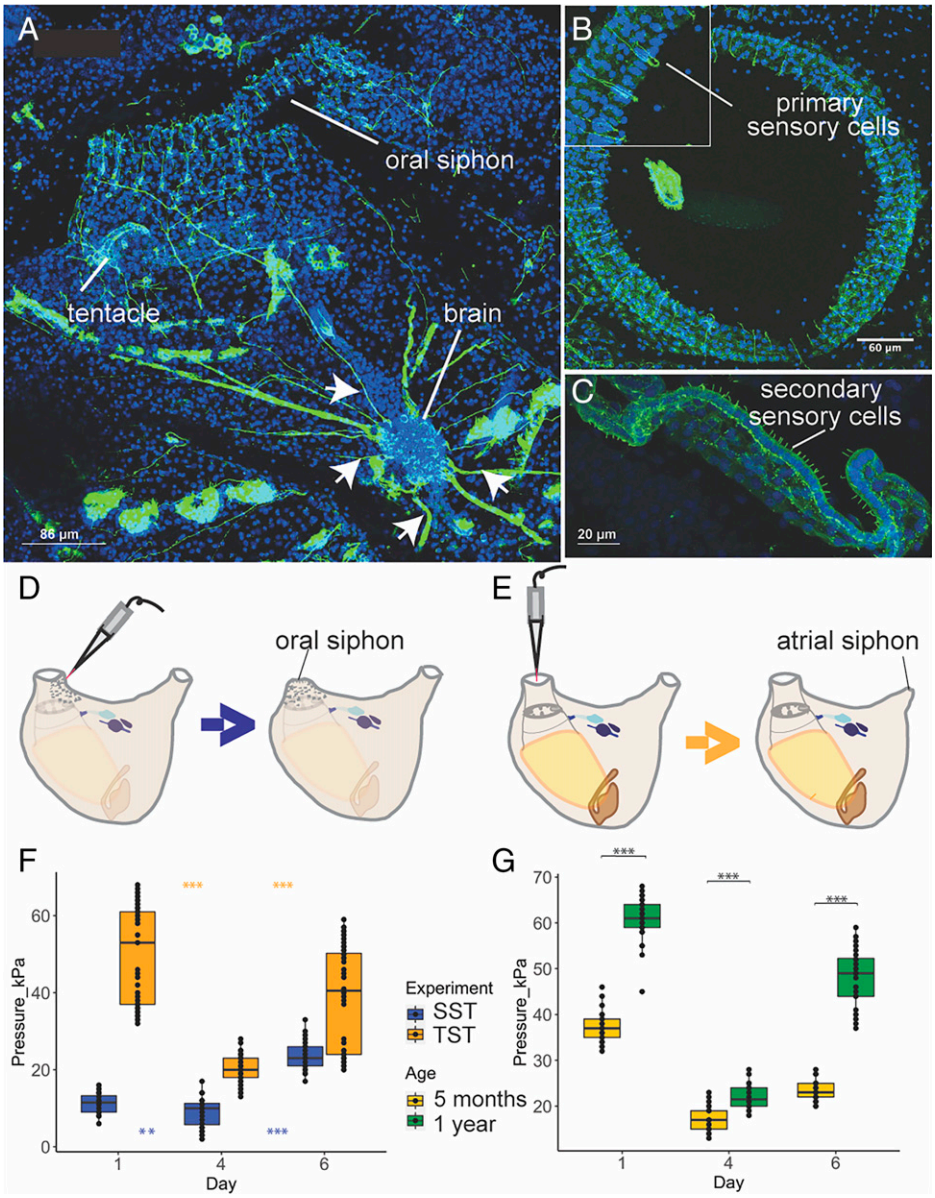

Fig. 4. Adult zooids behavioral response is impaired during both the weekly cycle and with age. *(A-C)* Confocal imaging nervous system stained with anti-alpha tubulin (green) and Hoechst (blue). *(A)* Dorsal view of an adult zooid. Nerves (arrows) branching from the brain toward the oral siphon are clearly visible. *(B)* Upper view of the oral siphon populated with primary sensory cells. These mechanoreceptor cells are in epidermis and have both a cilium (dendrite) and an axon directed to the brain. When stimulated they activate the oral siphon sphincter muscle contraction and induce siphon closure. *(C)* Tentacle, at the base of the oral siphon, with a row of secondary sensory cells (coronal cells). At their base, they form synapses with dendrites belonging to brain neurons. Their stimulation induces the contraction of both body and atrial siphon muscles, leading to expulsion of seawater from the oral siphon. *(D* and *E)* Experimental design of the behavioral tests. In the siphon stimulation test (SST) (*D*) a jet of seawater is used to stimulate the oral siphon primary sensory cells in epidermis. In the tentacle stimulation test (TST) (*E*), a jet of seawater stimulates the coronal cells of the tentacles. *(F)* Behavioral response of zooids following TSTs and SSTs performed in days 1.4.6. *(G)* Comparison of behavioral response of adults from young and old colonies following TSTs performed during the days 1,4,6. ANOVA and post hoc test. *P* value < 0.05 (*); *P* value < 0.01 (**); *P* value < 0.001 (***).

17-y-old colonies and found that the aged brains contain fewer cells (Fig. 3*F* and *SI Appendix, Supplementary Data 7*). Brains of younger colonies not only reach a significantly higher number of neurons throughout adult life but also exhibit the largest increases in neurons between early and midcycle (Fig. 3*F*). This age specific amplitude, and the fact that the maximum number of neurons observed in the older brains is significantly lower than the number of neurons observed in younger brains, most likely reflects a robust cell division and stem cell activity in young colonies versus reduced activity in old colonies. These results also point to an ancient link between the immune and nervous systems (32) suggesting a key role to the immune system in neurodegenerative diseases (33, 34).

To test if this reduction in neuron number affects the ability of the zooids to respond to mechanical stimuli, we developed 2 functional assays that measure zooid activity. The first stimulates the oral siphon primary sensory cells to induce oral siphon closure (35) and is called siphon stimulation test (SST) (Fig. 4 *A–B*, and *D*). The second stimulates secondary sensory cells (20) to induce the contraction of both zooid body and atrial siphon muscles (35) and is called tentacle stimulation test (TST) (36) (Fig. 4 *A*, *C*, and *E*). Using a waterjet controlled by a microinjector, we stimulated sensory cells and determined the minimum pressure needed to induce the contraction of the target siphons. Both functional assays revealed that brain neuron numbers correlate with siphon sensitivity to stimuli (highest in midcycle) (Fig. 4*F* and *SI Appendix, Supplementary Data 8*). We investigated if the differences in oral siphon sensitivity were correlated with changes in the number of primary sensory cells

during the weekly cycle and found that the number of oral siphon primary sensory cells tripled from early to midcycle before decreasing in late cycle, similar to the trend described for brain neurons (Figs. 3*G* and 4*B* and *SI Appendix*, *Supplementary Data 9*). The decrease in the number of both brain neurons and primary sensory cells during late cycle explains the reduced sensitivity to stimuli. Moreover, the comparison between the number of primary sensory cells in young and old colonies, shows a significant difference in day 6, with the lower number of sensory cells in old colonies (Fig. 3*G*).

To determine if fewer neurons and primary sensory cells affect the ability of a zooid to respond to stimuli, we compared the ability of old and young colonies to respond to the TST assay and found that old colonies are less sensitive and higher pressure is needed to evoke a response (Fig. 4*G* and *SI Appendix*, *Supplementary Data 10*). Even with more cells at day 1 (Fig. 3*F*), old colonies are less sensitive to touch. These results suggest that aging affects zooid sensitivity to stimuli.

Evolutionary Conserved Mechanisms of Neurodegeneration and Regeneration. To examine gene expression in the brain of *B. schlosseri* and identify molecular signatures potentially linked with development and degeneration phenotypes, we sequenced and analyzed the transcriptomes of the dissected neural complex of zooids at days 1, 4, and 6 in both young (5 mo, $n = 6$) and old colonies (7 to 16 y, $n = 5$). The neural complex was dissected (Fig. 5 *A* and *B*) and cDNA libraries were prepared for sequencing (RNA-seq) (2 × 150 bp reads, Illumina NextSEq. 500). Following quality control filters, reads were aligned to the *B. schlosseri* transcriptome (5) and gene counts determined (*SI Appendix*, *Supplementary Data 11–13*). A custom algorithm was used to identify genes that had differential expression (DE) between different days of the blastogenic cycle in young colonies (22).

Homologous genes that were significantly ($P < 0.05$) up-regulated or down-regulated in the enriched brain when comparing early versus late cycle and young versus old colonies, were analyzed in GeneAnalytics (37) (Fig. 5 *B* and *C* and *SI Appendix*, Fig. S7 and *Supplementary Data 14–16*). The genes significantly differentially expressed between the brains belonging to adult zooids at day 1 versus adult zooids at day 6 reveal the brain and its subgrouping cerebral cortex as the highest scores for the tissue category (with the shared expression of 350 genes in the brain of *B. schlosseri* and the human cerebral cortex), and the neuronal disease and its subgrouping disease of mental health as highest number of hits and score for the disease category (Fig. 5 *B* and *C* and *SI Appendix*, *Supplementary Data 17–19*).

To test whether the brains continue to develop in adult individual zooids and if apoptosis is involved in the neurodegenerative process, we calculated the relative enrichment for gene sets of genes associated with human central nervous system development and neuron apoptotic process with *B. schlosseri* homologies across the weekly cycle (Fig. 5 *E* and *F* and *SI Appendix*, *Supplementary Data 20*, see *Materials and Methods in the SI Appendix*). Briefly, the number of genes that are highly expressed each day are compared to random selections of genes to infer whether more or less of the genes are active than would be expected by chance. We found the CNS development gene enrichment (Fig. 5*E*) decreases from day 4 to day 6, with 128 genes highly expressed early in the cycle that are not in the late cycle. These include transcription factors involved in CNS development and adult tissue homeostasis and regeneration (*SOX2*, *SOX8*, *SOX9*, *PITX3*); genes involved in differentiation and proliferation (*NOTCH3*); neurogenesis (*NEUROG3*); neuron migration (*RELN*, *FGFR1*, *PRKG1*) and axon guidance (*SLIT2*). In the late cycle, 108 genes are highly expressed compared to the early cycle, including those related to cellular degradation (*UBB*), chromosome condensation (*NIPBL*), negative regulation of the ras signal transduction pathway (*NF1*), triggers for apoptosis through expression of genes necessary for cell death (*FOXO3*, *CASP2*, *CASP3*), and the mediation of growth factor-induced neuronal survival suppressing apoptosis (*AKT*). This enrichment pattern aligns with the increase in neuron number from days 1 to 4 (Fig. 3*B*). In contrast, the neuron death gene enrichment (Fig. 5*F*) increases from a zero baseline at day 3 to a positive enrichment on days 5 and 6. Genes possessing this expression pattern include those related to neuron apoptotic processes (*GRN*, *FOXO3*, *NF1*) and cellular accumulation of or response to amyloid-beta (*PSEN1*, *CDK5*, *CDK5R1*). This result further supports the presence of apoptotic neurons (*SI Appendix*, Figs. S2 and S3) in late cycle.

Genes associated with human neurodegenerative diseases (Alzheimer, Parkinson, Frontotemporal dementia, and Huntington) [source: MalaCard, Human Disease Database (37)] had 428 genes with putative homology in *B. schlosseri* that were expressed in its CNS. Differential expression analysis of brains between days 1 and 5 [DESEq. (38)] identified 73 DE genes (Fig. 5*G* and *SI Appendix*, *Supplementary Data 21*). Highly expressed in the late cycle are *APP* and *PARK2*, genes that in humans have variants linked to neurodegenerative disease. Following similar trends in human disease are *DNAH6*, *DNHD1*, *TNXB*, *SEMA6D*. These results were validated with qPCR on additional brains (Fig. 5 *H–K* and *SI Appendix*, *Supplementary Data 22*) with *APP*, *CDK5*, *CDK5R1* showing similar patterns of high expression in late cycle compared to early cycle. Additionally *LRP1* (clearance of apoptotic cells and amyloid precursor protein) is expressed throughout the cycle.

Given the decreased brain size of old zooids and their lowered response to stimuli, we hypothesize that gene expression changes in old colonies (7-16 y) compared to young (5 mo) may be associated with neurodegeneration and looked for homologs of genes that are associated with neurodegenerative diseases in humans. Indeed, we identified 148 such genes when comparing brains of different ages across all developmental stages (*SI Appendix*, *Supplementary Data 23*) and 104 when comparing the same developmental stage (Day 1) across ages (Fig. 6*A* and *SI Appendix*, *Supplementary Data 24*). Of these, those that are linked to genetic variants in humans include, *PINK1*, *TBP*, *VCP*; those that are linked to expression differences with diseases include, *TNS1*, *ANKS1B*, *FREM1*, *RGL3*, *SLIT1*, *UNC80*. A comparison of the 73 genes differentially expressed during the weekly blastogenic cycle and the 148 genes differentially expressed with aging revealed that 35 genes are shared, and 27 of them have a common trend (i.e., increasing or decreasing expression in late cycle and in old brains) (*SI Appendix*, Fig. S8). This is a significant ($P < 0.01$, binomial test) number of genes sharing the same pattern. A hypergeometric model of the number of genes that are DE in each process (73 and 148 out of 428) with the number that were found to overlap (35) shows a statistically significant association ($P <$ 1e-2). This suggests that these two neurodegeneration processes share transcriptional programs. Aging related to neurodegeneration is well correlated with neuroinflammation in humans (39, 40). 28 genes that are associated with neuroinflammation and inflammation pathways (29, 41) are expressed in the *B. schlosseri* brain. Among them 19 are differentially expressed between young and old colonies including IL17, NFKB, Caspases, C3, NLRC, and TNFalpha (*SI Appendix*, *Supplementary Data 25*).

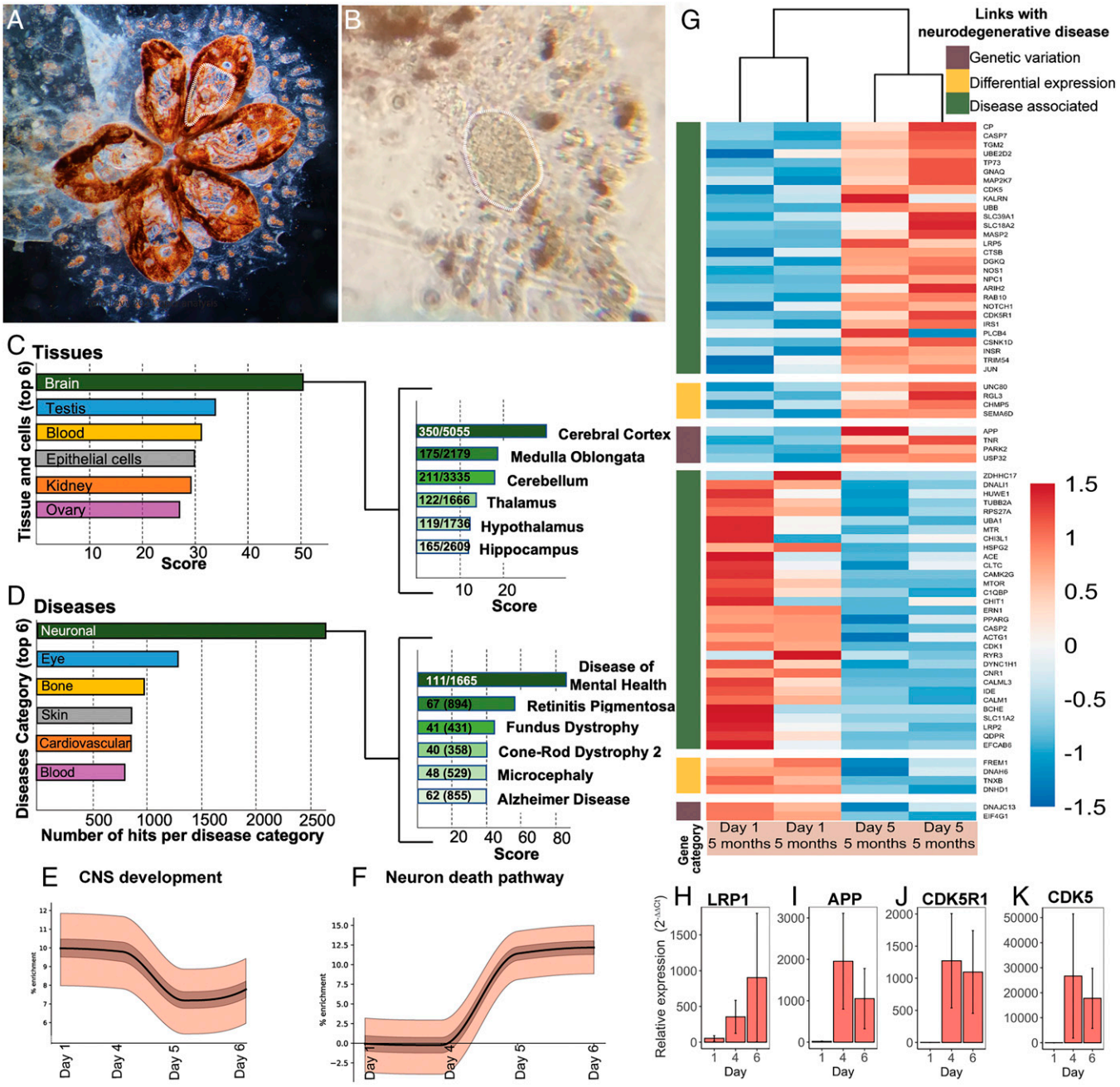

Fig. 5. Significant changes in the expression of genes associated with mammalian neurodegeneration pathways are observed during the weekly degeneration cycles. *(A)* Colony after brain dissection. White dotted lines highlight tissues removed. *(B)* Extracted brain. *(C* and *D)* Analysis with GeneAnalytics of differentially expressed genes between early and late cycle in the enriched brain of *B. schlosseri* (RNA-seq). *(C)* Tissues and cell categories and (*B*) diseases associated with differentially expressed genes. For each panel, only the 6 categories with the highest score and number of hits per category are displayed (the complete lists can be found in *SI Appendix, Supplementary Data 14–16*). *Right* identifies the subgroupings which the contribute to the dominant category (i.e., the Brain for Tissues and Cells and Neuronal for Disease), with the numeric ratio describing the number of genes detected in *B. schlosseri* as compared to the total number of genes associated with the subgrouping within the database. In all cases, x-axis scores refer to the weighted sum of the scores of all matched genes in this category, normalized to the log of the maximal score that can be achieved for the category. *(E* and *F)* Enrichment plots showing increase in proportion of genes associated with the CNS development (*E*) and neuronal death pathway (*F*). The solid line is the proportion of active selected genes with the expected mean subtracted. Light and dark bands correspond to 50% and 99% confidence intervals, respectively. *(G)* Seventy-three putative homologous genes associated with neurodegenerative diseases are DE in the zooid brain during the weekly cycle. Categories are indicated based on the link that the gene has with the neurodegenerative disease (brown: genes having a genetic variation in patients with the disease; yellow: genes DE in patients with the diseases compared to the healthy controls; green: genes identified by scientific literature, cancer mutation data, and genome-wide association studies). Color scale depicts $\log_2$CPM normalized expression values scaled by row. *(H–K)* qPCR expression of selected genes on brain tissue. APP: amyloid precursor protein, CDK5: cyclin-dependent kinase 5, LRP1: low-density lipoprotein receptor related protein1, CDK5R1: cyclin dependent kinase 5 activator 1; error bars represent SEMs.

Unlike most species where the body is long-lived and maintained by cellular replacements, a *B. schlosseri* colony regenerates new zooids on a weekly basis and its stem cells persist for its entire life (1). Putative adult stem cells mediate bud development (7, 8, 30, 42) and recent transcriptome analyses suggest that these stem cells are tissue specific (22). For this reason, we investigated the genes included in the mammalian neural stem cell (NSC) and lineage-specific pathway (37) and found that 27 putative homologous genes are expressed in *B. schlosseri* brain (Fig. 6*B* and *SI Appendix, Supplementary Data 26*). Among

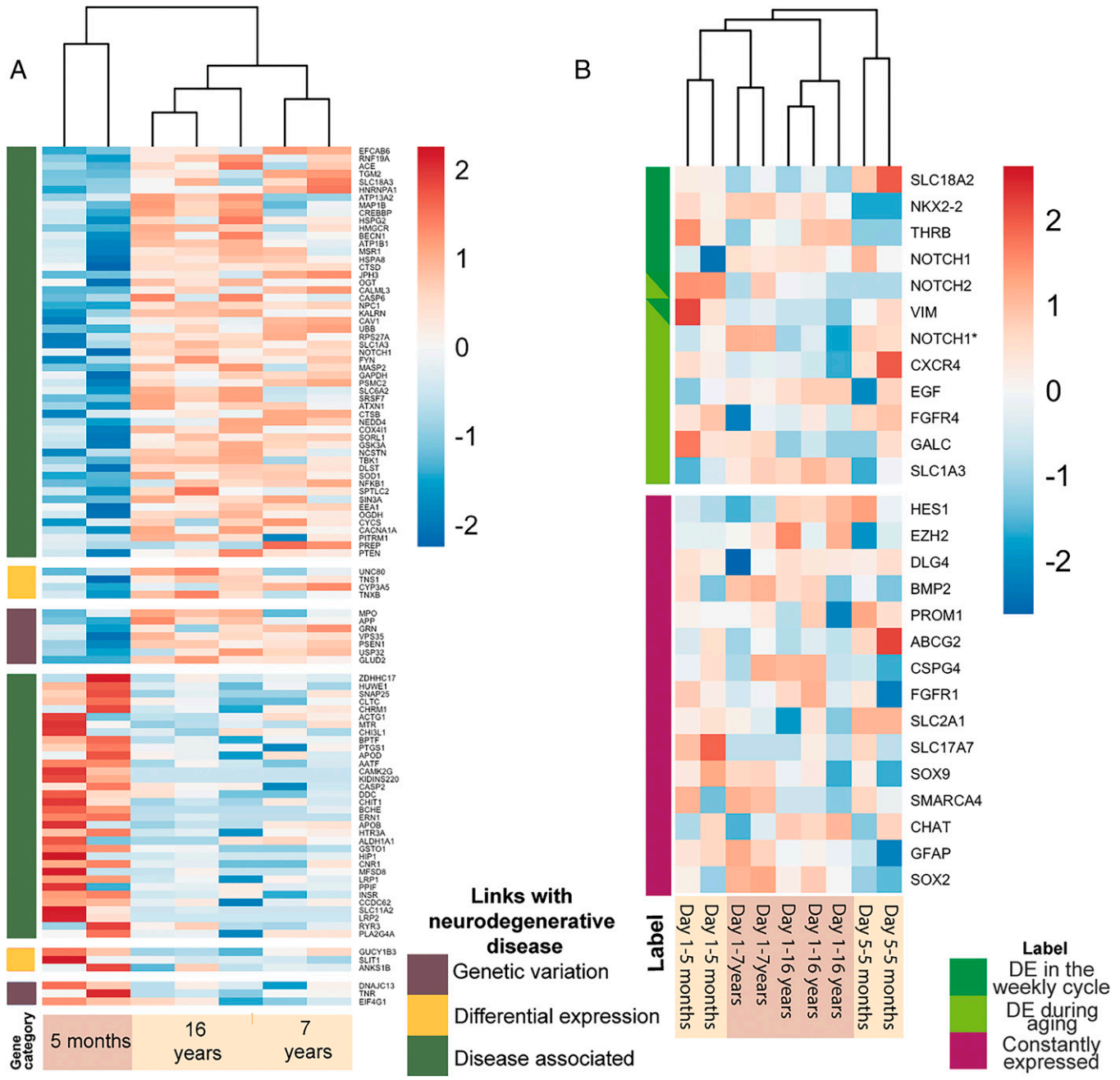

Fig. 6. Significant changes in the expression of genes associated with mammalian neural stem cells and neurodegeneration pathways are observed during aging. *(A)* DE putative homologous genes associated with neurodegenerative disease are DE in zooid's brain belonging to colonies with different ages (young: 5 mo; old: 7 and 16 y). Categories are indicated based on the link that the gene has with the neurodegenerative disease (brown: genes having a genetic variation in patients with the disease; yellow: genes DE in patients with the diseases compared to the healthy controls; green: genes identified by scientific literature, cancer mutation data, and genome-wide association studies). *(B)* Putative homologous genes associated with mammal neural stem cells are expressed in zooid brains belonging to colonies of different ages (young: 5 mo; old: 7 and 16 y) and in brains at day 1 and 5 of the weekly cycle. Color scales depicts log_2CPM normalized expression values scaled by row. *Indicates different sequences that are putative homologous to the same gene.

them, 6 are DE within the blastogenic cycle (*NKX2-2*, *THRB*, *VIM*, *NOTCH1*, *NOTCH2*, *SLC18A2*) and 8 are DE between young and old colonies (*CXCR4*, *FGFR4*, *CALC*, *VIM*, *EGF*, *NOTCH1*, *SLC1A3*) (*SI Appendix*, Fig. S9). In human fetal NSC subsets of cells shown to migrate long distances before differentiating and maturing express CXCR4 (43), the chemokine receptor for CXCL12, potentially indicating the migrating subset in *B. schlosseri*. These data reveal the existence of both dynamic and continuous neural stem cell activity in the brain across both timescales. The study of these genes might point to key regulators of NSCs in aging.

Discussion

Here we introduce *B. schlosseri* as a model for evolutionary neuroscience. As an organism belonging to the closest relative clade to vertebrates whose life cycle is characterized by 2 distinct (i.e., short-term and long-term) yet apparently related neurodegenerative pathways, we suggest that this colonial tunicate offers unique opportunities for novel research concerning neurogenesis, neural degeneration, aging, and loss of nervous system function. Our investigation reveals dramatic changes in cell type, cell number, and brain structure during weekly budding cycles and with

colony aging. These changes are associated with 1) impaired sensorial ability as inferred by behavioral simulation tests and 2) the differential expression of 186 unique (and 35 common) putative genes with mammalian homologs associated with human neurodegenerative diseases and the differential expression of 12 unique putative genes associated with neural stem cells. Importantly, these lists include genes whose genetic variation predicts the onset of neurodegenerative diseases in humans through mechanisms and pathways that future research, building upon these foundational descriptions, will be well positioned to investigate.

A Colonial Tunicate Model for Neuroscience. Tunicates like *B. schlosseri* represent the earliest chordate lineage (18). Advanced transgenic lineage tracing and single-cell transcriptome trajectories studies on the embryonic development of the solitary tunicate *Ciona* species, have previously provide insight into the evolution of the development of the nervous system (44–49). With studies documenting its incredible regenerative capacities, *Ciona* has also been advanced as a model to study aging and regeneration and the relationship between them (50). While solitary tunicate species reproduce sexually through embryogenesis, colonial tunicates like *B. schlosseri* reproduce through a weekly budding cycle (i.e., asexual reproduction) in addition to embryogenesis (i.e., sexual reproduction). The asexual reproductive pathway of *B. schlosseri* provides an innovative platform to study the function of gene products that affect cyclical brain regeneration and degeneration. Moreover, this colonial tunicate can be reared in laboratory conditions for more than 20 y, providing the unique opportunity to study the effects of aging (17). Studies in sea urchin and mollusk transcriptomes have identified comparable mechanisms for aging (51, 52) and studies in short-lived invertebrate and vertebrate transgenic model organisms like yeast, flies, and nematodes, and fish have revealed conserved molecular and cellular mechanisms implicated in neurodegenerative diseases (53–57). While in the latter studies neurodegeneration was artificially induced, our study highlights *B. schlosseri* as an organism with a life history that includes naturally occurring neurodegeneration in a pair (i.e., short-term and long-term) of distinct but connected pathways.

Changes in Neural Number and Function with Age and Developmental Stage. In *B. schlosseri*, the CNS, sensory cells, and associated behavioral responses change dynamically over the course of adult zooid life. Our investigation reveals that the brain is not stable in cell number, which increases during the first phases of the cycle and then decreases before the brain is totally resorbed at the takeover stage. This finding raises new questions about the processes of adult neurogenesis and neurodegeneration, and the origin of different cell types within the neural complex. 3D reconstructions reveal that the relationship between the brain and the other components of the neural complex (i.e., dorsal organ and neural gland) changes alongside the number neurons during the weekly budding cycle. Therefore, as others have suggested previously (58), we believe it likely that these organs have an active role in adult neurogenesis. Apoptosis occurs in the brain, suggesting that this cell death mechanism plays a role in tissue modeling not only during bud development and takeover (23, 59, 60) but also during adult life. Indeed, specific trends in brain cell number are likely a product of the dynamic balance between brain cell death and neurogenesis that varies with developmental stage and age. We also investigated immunocytes (morula cells and phagocytes) with and around the brain, finding that their number increases significantly during the weekly cycle. Immunocytes could play an important role during neurodegeneration, that may be ascribed to their known roles in cytotoxicity (morula cells) and clearance activity (phagocytes) (30, 61). The trend in brain neuron number that we documented correlates with that of oral siphon epidermal receptors. In both cases, the highest number of cells is found at mid cycle (day 4). Accumulated evidence indicates that these trends impact animal performance. The behavioral tests (SST and TST) that we developed showed that zooid response to mechanical stimulation of oral siphon epidermal receptors and coronal cells varied during the cycle. The phase with the highest number of neurons and sensory cells (midcycle) represents the highest animal sensitivity, whereas the phase with the lowest number of neurons and sensory cells represents the lowest sensitivity.

Evolutionary Conserved Molecular Signatures of Neurogenesis, Neurodegeneration, and Aging. We also demonstrate the utility of this species as a model for analyzing the genetic basis of aging and loss of nervous system function. These processes within *B. schlosseri* may be linked to those within mammals on account of the extensive number of CNS genes homologous to human and mouse genes associated with neurodegenerative diseases. We found a significant differential expression of these genes between young and old colonies that have been associated with mammalian aging (62) and the accumulation of pathogenic elements over time at the genetic, molecular, cellular, and functional levels (63). Specifically, clear patterns of differentially expressed genes associated with human neurodegenerative diseases like Alzheimer, Parkinson, and frontotemporal dementia are evident between young and old colonies alongside age-related phenotypes associated with lower brain cell number, lower sensory cell number, and worse behavioral performance. Aging of a colony is, by definition, aging of its stem cells as most other cells are generated from these stem cells on a weekly basis (1). In adult mammalian tissues, stem cells are stably maintained in their niche throughout most, if not all, of an organism's life, although in humans and mice at least two subsets of hematopoietic stem cells exist, a balanced or lymphoid biased subset that dominates in youth, and a myeloid biased, proinflammatory subset that dominates in aging (64–66). In *B. schlosseri* although somatic tissues undergo weekly waves of apoptosis and phagocytosis, colonies undergo regeneration and live for years. Repeated trafficking of stem cells into new niches prevents their destruction by degenerating and/or stiffening tissues, as has been documented in mammalian systems (67), and enables self-preservation throughout life, perhaps via homing receptors and chemokine receptors (1, 68). Based upon recent transcriptomic analysis that suggest the existence of tissue-specific stem cells in *B. schlosseri* (22), we investigated the expression of neural stem cell genes in the neural complex of *B. schlosseri* during the weekly cycle and with age. We identified 15 genes that were constantly expressed as compared to 6 genes differentially expressed within the blastogenetic cycle and 8 differentially expressed with age.

Final Observations. In this study we focused on the asexually reproductive phase of *Botryllus* life history, analogous to the stem cell-based regeneration of solitary species. Germline (4, 69) and somatic (7, 8, 70) stem cell competitions are enabled by the weekly early appearance of stem cells in buds and the exchange of stem cells via anastomosed extracorporeal blood vessels that make them colonial. It is likely that developmentally regulated cell trafficking receptors and ligands control early bud appearance and subsequent organogenesis. We have also noted that the sexually reproduced larval tadpole has a second brain (22); elsewhere we show that it likely receives sensory input from at least the tadpole specific photolith, and transmits motor signals to the tadpole

musculature to allow appropriate settlement and cosettlement just prior to metamorphosis and transition to colonial and asexually reproductive stages in its life history. Given the links between alterations in motor neuron strength and excitability and neurodegenerative diseases associated with loss of muscle function in mammalian species (i.e., amyotrophic lateral sclerosis) (71), subsequent analyses of motor neuron phenotypes in *B. schlosseri* may be particularly valuable. In the future, isolation of single candidate neural stem cells and their progeny at different phases of chordate and invertebrate development and takeover will be aided by single cell RNAseq and other single cell assays of selective gene activity and silencing, and could reveal the forerunners of the mammalian nervous system as well. Morpholino anti-sense or siRNAi (silencing RNA) will be used to test the loss of function for some of the candidate genes involved during the weekly neurodegeneration cycle to understand how this influences programmed cell death. Moreover single cell RNAseq on the macrophages associated with the brain will help to illuminate their role in development and degeneration. These studies may help elucidate cellular diversity within the neural complex, reveal the protective ligands that enable their migration to newly forming buds in the face of massive cell death and phagocytosis, and identify their functional role within neurogeneration and neurodegeneration. We believe that *B. schlosseri*, given its cyclical blastogenesis and semitransparent tissue, represents a robust, assayable, and repeatable model to study such mechanisms over very short (i.e., weekly) timescales and how the balance between them may vary with time and age at a fine scale. Indeed, given such features we advance *B. schlosseri* as a model capable of providing unique and fundamental insight to the field of evolutionary neuroscience.

Materials and Methods

Animals. Specimens of *Botryllus schlosseri* (family Botryllidae, order Stolidobranchiata) used in this study were collected from Venice Lagoon (Italy) and Monterey Bay (United States). They were reared adhering to glass according to Sabbadin's technique (72) at a constant temperature of 18 °C. As facilitated by the transparency of colony vasculature, the daily development of buds and zooids was monitored in vivo under the stereomicroscope to select the appropriate stages. The colonies were observed during both the larval period and the metamorphoses period to assign them an exact age.

Confocal Microscopy. A whole mount immunohistochemical method was combined with confocal microscopy and applied to colonies at selected stages. Further details are described in *SI Appendix, Materials and Methods*.

Electron Microscopy. Colonies at selected stages were fixed, dehydrated, embedded in Epon-Araldite resin and cut in ultra-thin sections (80 nm thick). Further details are described in *SI Appendix, Materials and Methods*.

3D Reconstruction. Five samples belonging to the same colony, fixed at four different colony phases (late bud stage, day 1, 4, 6, and 7), were embedded in resin and serially cut using a Histo Jumbo Knife (Diatome). One-micrometer thick sections were arranged in chains of ∼20 sections each and stained with toluidine blue. The neural complex was serially photographed and Amira software was used to create 3D reconstructions.

Apoptosis Detection. Sections (7 mm thick) were obtained with a Leitz 1212 microtome and used to detect apoptosis with the TUNEL reaction. Further details are described in *SI Appendix, Materials and Methods*.

Behavior Tests. Relying on methods described in earlier work (35), we performed two behavioral tests: the siphon stimulation test (SST) and the tentacle stimulation test (TTS). The first test involved the stimulation of the oral siphon epidermal receptors, i.e., primary sensory cells located in the oral siphon wall, whereas the TTS involved the stimulation of the coronal cells, i.e., the secondary sensory cells of the oral tentacles. Further details are described in *SI Appendix, Materials and Methods*.

Statistics. Statistical analyses were performed using R software environment version 4.0.1 (73). Further details are described in *SI Appendix, Materials and Methods*.

qPCR. qPCR were performed on brains removed from the colonies at selected stages as identified in the main text. Further details are described in *SI Appendix, Materials and Methods*.

Transcriptomes and Gene Analysis. Enriched neural complex were dissected from the adult zooids at selected stages and ages. In addition to neurons the dissected tissues include blood cells, immunocytes and tunic cells found in close proximity to the neural complex (Fig. 5*B*). We used the protocol described in Voskoboynik et al., 2013 (5) to extract RNA from the brains at the stages and ages identified in the main text. cDNA libraries were then prepared from high quality samples (RIN > 8) using Ovation RNA-seq v2 (Nugen). Barcoded library samples were then sequenced on an Illumina NextSEq. **500**. Gene homology was determined based on genome annotation. Gene count information was imported into R and differential expression between the two groups comprising each comparison was performed using Deseq2 (38) where genes with a P value <0.05 were characterized as being differentially expressed. Further details are described in *SI Appendix, Materials and Methods*.

Data Availability. RNA-seq data are available on the Sequence Read Archive (SRA) database: BioProject: PRJNA732987. RNA-seq data have been deposited in [BioProject] (PRJNA732987) (https://www.ncbi.nlm.nih.gov/search/all/?term=%20PRJNA732987) (74). All study data are included in the article and/or *SI Appendix*.

ACKNOWLEDGMENTS. We thank L. Ballarin, P. Burighel, G. Zaniolo, T. Frawley, E. Greggio, M. Zordan, T. Stach, S. Thompson, P. Bump, J. Lopez, C. Lowe, F. Cima, Y. Voskoboynik, and A. Glina for technical advice and helpful discussion. Thanks to P. Sartori, A. Targonato, V. Giusti, B. Meneghetti and L. Morin for helping in collecting data. This study was supported by NIH grants R01AG037968 and RO1GM100315 to I.L.W., S.R.Q., and A.V., and by R21AG062948 to I.L.W. and A.V. the Chan Zuckerberg investigator program to S.R.Q., I.L.W., and A.V, the Stinehart-Reed grant to I.L.W. and A.V., the grant from the University of Padova, Progetti di Ricerca di Ateneo (Grant 2015–CPDA153837) by L.M., F.G., and F.C. C.A. was supported by Larry L. Hillblom foundation Postdoctoral Fellowship, by Stanford School of Medicine Dean's Postdoctoral Fellowship, Aldo Gini Foundation Fellowship and Iniziative di Cooperazione Universitaria 2017 Fellowship of the University of Padova.

Author affiliations: [a]Stanford University, Hopkins Marine Station, Pacific Grove, CA 93950; [b]Institute for Stem Cell Biology and Regenerative Medicine, Stanford University School of Medicine, Stanford, CA 94305; [c]Department of Physics, Stanford University, Stanford, CA 94305; [d]Dipartimento di Biologia, Università degli Studi di Padova, 35131, Padova, Italy; [e]Chan Zuckerberg Biohub, San Francisco CA 94158; [f]Departments of Applied Physics and Bioengineering, Stanford University, Stanford, CA 94305; and [g]Department of Biology, Stanford University, Hopkins Marine Station, Pacific Grove, CA 93950

1. A. Voskoboynik, I. L. Weissman, *Botryllus schlosseri*, an emerging model for the study of aging, stem cells, and mechanisms of regeneration. *Invertebr. Reprod. Dev.* **59** (suppl. 1), 33–38 (2015).
2. L. Manni *et al.*, Sixty years of experimental studies on the blastogenesis of the colonial tunicate Botryllus schlosseri. *Dev. Biol.* **448**, 293–308 (2019).
3. V. L. Scofield, J. M. Schlumpberger, L. A. West, I. L. Weissman, Protochordate allorecognition is controlled by a MHC-like gene system. *Nature* **295**, 499–502 (1982).
4. D. S. Stoner, B. Rinkevich, I. L. Weissman, Heritable germ and somatic cell lineage competitions in chimeric colonial protochordates. *Proc. Natl. Acad. Sci. U.S.A.* **96**, 9148–9153 (1999).
5. A. Voskoboynik *et al.*, The genome sequence of the colonial chordate, Botryllus schlosseri. *eLife* **2**, e00569 (2013).
6. B. Rosental, T. Raveh, A. Voskoboynik, I. L. Weissman, Evolutionary perspective on the hematopoietic system through a colonial chordate: Allogeneic immunity and hematopoiesis. *Curr. Opin. Immunol.* **62**, 91–98 (2020).
7. D. J. Laird, A. W. De Tomaso, I. L. Weissman, Stem cells are units of natural selection in a colonial ascidian. *Cell* **123**, 1351–1360 (2005).
8. A. Voskoboynik *et al.*, Identification of the endostyle as a stem cell niche in a colonial chordate. *Cell Stem Cell* **3**, 456–464 (2008).

9. R. K. Grosberg, Life-history variation within a population of the colonial ascidian Botryllus schlosseri. I. The genetic and environmental control of seasonal variation. *Evolution* **42**, 900–920 (1988).
10. N. E. Chadwick-Furman, I. L. Weissman, Life histories and senescence of Botryllus schlosseri (Chordata, Ascidiacea) in Monterey Bay. *Biol. Bull.* **189**, 36–41 (1995).
11. N. E. Chadwick-Furman, I. L. Weissman, Life history plasticity in chimaeras of the colonial ascidian Botryllus schlosseri. *Proc. Biol. Sci.* **262**, 157–162 (1995).
12. F. Cima *et al.*, Life history and ecological genetics of the colonial ascidian Botryllus schlosseri. *Zool. Anz.* **257**, 54–70 (2015).
13. A. Sabbadin, The compound ascidian Botryllus-schlosseri in the field and in the laboratory. *Pubbl. Stn. Zool. Napoli* **37**, 62–72 (1969).
14. H. C. Boyd, S. K. Brown, J. A. Harp, I. L. Weissman, Growth and sexual maturation of laboratory-cultured monterey *Botryllus schlosseri*. *Biol. Bull.* **170**, 91–109 (1986).
15. B. Rinkevich, R. J. Lauzon, B. W. Brown, I. L. Weissman, Evidence for a programmed life span in a colonial protochordate. *Proc. Natl. Acad. Sci. U.S.A.* **89**, 3546–3550 (1992).
16. R. J. Lauzon, B. Rinkevich, C. W. Patton, I. L. Weissman, A morphological study of nonrandom senescence in a colonial urochordate. *Biol. Bull.* **198**, 367–378 (2000).
17. Y. Voskoboynik *et al.*, Global age-specific patterns of cyclic gene expression revealed by tunicate transcriptome atlas. bioRxiv (2020). https://doi.org/10.1101/2020.12.08.417055 Accessed April 11 2022.
18. F. Delsuc, H. Brinkmann, D. Chourrout, H. Philippe, Tunicates and not cephalochordates are the closest living relatives of vertebrates. *Nature* **439**, 965–968 (2006).
19. P. Burighel, N. J. Lane, G. Zaniolo, L. Manni, Neurogenic role of the neural gland in the development of the ascidian, Botryllus schlosseri (Tunicata, Urochordata). *J. Comp. Neurol.* **394**, 230–241 (1998).
20. P. Burighel, M. Sorrentino, G. Zaniolo, M. C. Thorndyke, L. Manni, The peripheral nervous system of an ascidian, Botryllus schlosseri, as revealed by cholinesterase activity. *Invertebr. Biol.* **120**, 185–198 (2001).
21. L. Manni, R. Pennati, "Tunicata" in *Structure and Evolution of Invertebrate Nervous Systems*, A. Schmidt-Rhaesa, S. Harzsch, G. Purschke, Eds. (Oxford University Press, 2015), pp. 699–718.
22. M. Kowarsky *et al.*, Sexual and asexual development: Two distinct programs producing the same tunicate. *Cell Rep.* **34**, 108681 (2021).
23. L. Ballarin, F. Schiavon, L. Manni, Natural apoptosis during the blastogenetic cycle of the colonial ascidian Botryllus schlosseri: A morphological analysis. *Zool. Sci.* **27**, 96–102 (2010).
24. S. A. Arkett, G. O. Mackie, C. L. Singla, Neuronal organization of the ascidian (Urochordata) branchial basket revealed by cholinesterase activity. *Cell Tissue Res.* **257**, 285–294 (1989).
25. G. O. Mackie, R. C. Wyeth, Conduction and coordination in deganglionated ascidians. *Can. J. Zool.* **78**, 1626–1639 (2000).
26. G. Zaniolo, N. J. Lane, P. Burighel, L. Manni, Development of the motor nervous system in ascidians. *J. Comp. Neurol.* **443**, 124–135 (2002).
27. K. Braun, T. Stach, Morphology and evolution of the central nervous system in adult tunicates. *J. Zool. Syst. Evol. Res.* **57**, 323–344 (2019).
28. S. Tiozzo, M. Murray, B. M. Degnan, A. W. De Tomaso, R. P. Croll, Development of the neuromuscular system during asexual propagation in an invertebrate chordate. *Dev. Dyn.* **238**, 2081–2094 (2009).
29. D. M. Corey *et al.*, Developmental cell death programs license cytotoxic cells to eliminate histocompatible partners. *Proc. Natl. Acad. Sci. U.S.A.* **113**, 6520–6525 (2016).
30. B. Rosental *et al.*, Complex mammalian-like haematopoietic system found in a colonial chordate. *Nature* **564**, 425–429 (2018).
31. A. Peronato *et al.*, Complement system and phagocytosis in a colonial protochordate. *Dev. Comp. Immunol.* **103**, 103530 (2020).
32. A. Kraus, K. M. Buckley, I. Salinas, Sensing the world and its dangers: An evolutionary perspective in neuroimmunology. *eLife* **10**, e66706 (2021).
33. V. A. Pavlov, K. J. Tracey, Neural regulation of immunity: Molecular mechanisms and clinical translation. *Nat. Neurosci.* **20**, 156–166 (2017).
34. J. V. Pluvinage, T. Wyss-Coray, Systemic factors as mediators of brain homeostasis, ageing and neurodegeneration. *Nat. Rev. Neurosci.* **21**, 93–102 (2020).
35. G. O. Mackie, P. Burighel, F. Caicci, L. Manni, Innervation of ascidian siphons and their responses to stimulation. *Can. J. Zool.* **84**, 1146–1162 (2006).
36. L. Manni, C. Anselmi, P. Burighel, M. Martini, F. Gasparini, Differentiation and induced sensorial alteration of the coronal organ in the asexual life of a tunicate. *Integr. Comp. Biol.* **58**, 317–328 (2018).
37. S. Ben-Ari Fuchs *et al.*, Geneanalytics: An integrative gene set analysis tool for next generation sequencing, RNAseq and microarray data. *OMICS* **20**, 139–151 (2016).
38. M. I. Love, W. Huber, S. Anders, Moderated estimation of fold change and dispersion for RNA-seq data with DESeq2. *Genome Biol.* **15**, 550 (2014).
39. R. M. McManus, M. T. Heneka, Role of neuroinflammation in neurodegeneration: New insights. *Alzheimers Res. Ther.* **9**, 14 (2017).
40. R. M. Ransohoff, How neuroinflammation contributes to neurodegeneration. *Science* **353**, 777–783 (2016).
41. T. Shabab, R. Khanabdali, S. Z. Moghadamtousi, H. A. Kadir, G. Mohan, Neuroinflammation pathways: A general review. *Int. J. Neurosci.* **127**, 624–633 (2017).
42. Y. Rinkevich *et al.*, Repeated, long-term cycling of putative stem cells between niches in a basal chordate. *Dev. Cell* **24**, 76–88 (2013).
43. M. Drukker *et al.*, Isolation of primitive endoderm, mesoderm, vascular endothelial and trophoblast progenitors from human pluripotent stem cells. *Nat. Biotechnol.* **30**, 531–542 (2012).
44. S. Sharma, W. Wang, A. Stolfi, Single-cell transcriptome profiling of the Ciona larval brain. *Dev. Biol.* **448**, 226–236 (2019).
45. S. Gibboney *et al.*, Effector gene expression underlying neuron subtype-specific traits in the motor ganglion of Ciona. *Dev. Biol.* **458**, 52–63 (2020).
46. E. K. Farley *et al.*, Suboptimization of developmental enhancers. *Science* **350**, 325–328 (2015).
47. E. K. Farley, K. M. Olson, W. Zhang, D. S. Rokhsar, M. S. Levine, Syntax compensates for poor binding sites to encode tissue specificity of developmental enhancers. *Proc. Natl. Acad. Sci. U.S.A.* **113**, 6508–6513 (2016).
48. V. Bertrand, C. Hudson, D. Caillol, C. Popovici, P. Lemaire, Neural tissue in ascidian embryos is induced by FGF9/16/20, acting via a combination of maternal GATA and Ets transcription factors. *Cell* **115**, 615–627 (2003).
49. A. Stolfi, K. Ryan, I. A. Meinertzhagen, L. Christiaen, Migratory neuronal progenitors arise from the neural plate borders in tunicates. *Nature* **527**, 371–374 (2015).
50. W. R. Jeffery, Regeneration, stem cells, and aging in the Tunicate Ciona: Insights from the oral siphon. *Int. Rev. Cell Mol. Biol.* **319**, 255–282 (2015).
51. J. M. Polinski, N. Kron, D. R. Smith, A. G. Bodnar, Unique age-related transcriptional signature in the nervous system of the long-lived red sea urchin Mesocentrotus franciscanus. *Sci. Rep.* **10**, 9182 (2020).
52. J. B. Greer, M. C. Schmale, L. A. Fieber, Whole-transcriptome changes in gene expression accompany aging of sensory neurons in Aplysia californica. *BMC Genomics* **19**, 529 (2018).
53. L. M. Thompson, J. L. Marsh, Invertebrate models of neurologic disease: Insights into pathogenesis and therapy. *Curr. Neurol. Neurosci. Rep.* **3**, 442–448 (2003).
54. S. Rencus-Lazar, Y. DeRowe, H. Adsi, E. Gazit, D. Laor, Yeast models for the study of amyloid-associated disorders and development of future therapy. *Front. Mol. Biosci.* **6**, 15 (2019).
55. A. Surguchov, Invertebrate models untangle the mechanism of neurodegeneration in Parkinson's disease. *Cells* **10**, 407 (2021).
56. I. Harel *et al.*, A platform for rapid exploration of aging and diseases in a naturally short-lived vertebrate. *Cell* **160**, 1013–1026 (2015).
57. X. Wang, J.-B. Zhang, K.-J. He, F. Wang, C.-F. Liu, Advances of zebrafish in neurodegenerative disease: From models to drug discovery. *Front. Pharmacol.* **12**, 713963 (2021).
58. M. M. Prünster, L. Ricci, F. D. Brown, S. Tiozzo, De novo neurogenesis in a budding chordate: Co-option of larval anteroposterior patterning genes in a transitory neurogenic organ. *Dev. Biol.* **448**, 342–352 (2019).
59. F. Cima *et al.*, Hovering between death and life: Natural apoptosis and phagocytes in the blastogenetic cycle of the colonial ascidian Botryllus schlosseri. *Dev. Comp. Immunol.* **34**, 272–285 (2010).
60. S. Tiozzo, L. Ballarin, P. Burighel, G. Zaniolo, Programmed cell death in vegetative development: Apoptosis during the colonial life cycle of the ascidian Botryllus schlosseri. *Tissue Cell* **38**, 193–201 (2006).
61. N. Franchi, L. Ballarin, Immunity in protochordates: The tunicate perspective. *Front. Immunol.* **8**, 674 (2017).
62. C. López-Otín, M. A. Blasco, L. Partridge, M. Serrano, G. Kroemer, The hallmarks of aging. *Cell* **153**, 1194–1217 (2013).
63. Y. Hou *et al.*, Ageing as a risk factor for neurodegenerative disease. *Nat. Rev. Neurol.* **15**, 565–581 (2019).
64. I. Beerman *et al.*, Functionally distinct hematopoietic stem cells modulate hematopoietic lineage potential during aging by a mechanism of clonal expansion. *Proc. Natl. Acad. Sci. U.S.A.* **107**, 5465–5470 (2010).
65. W. W. Pang *et al.*, Human bone marrow hematopoietic stem cells are increased in frequency and myeloid-biased with age. *Proc. Natl. Acad. Sci. U.S.A.* **108**, 20012–20017 (2011).
66. Y. Zhou, M. Lewallen, T. Xie, Stem cells' exodus: A journey to immortality. *Dev. Cell* **24**, 113–114 (2013).
67. M. Segel *et al.*, Niche stiffness underlies the ageing of central nervous system progenitor cells. *Nature* **573**, 130–134 (2019).
68. W. M. Gallatin, I. L. Weissman, E. C. Butcher, A cell-surface molecule involved in organ-specific homing of lymphocytes. 1983. *J. Immunol.* **177**, 5–9 (2006).
69. D. S. Stoner, I. L. Weissman, Somatic and germ cell parasitism in a colonial ascidian: Possible role for a highly polymorphic allorecognition system. *Proc. Natl. Acad. Sci. U.S.A.* **93**, 15254–15259 (1996).
70. I. Weissman, Evolution of normal and neoplastic tissue stem cells: Progress after Robert Hooke. *Philos. Trans. R. Soc. Lond. B Biol. Sci.* **370**, 20140364 (2015).
71. K. W. Kelley *et al.*, Kir4.1-dependent astrocyte-fast motor neuron interactions are required for peak strength. *Neuron* **98**, 306–319.e7 (2018).
72. A. Sabbadin, Osservazioni sullo sviluppo, l'accrescimento e la riproduzione di Botryllus schlosseri (Pallas), in condizioni di laboratorio. *Bolletino di zoologia* **22**, 243–263 (1955).
73. R Core Team, R: A language and environment for statistical computing (2021). R Foundation for Statistical Computing, Vienna, Austria. URL https://www.R-project.org./ Accessed April 11 2022.
74. C. Anselmi *et al.*, Botryllus schlosseri brain transcriptome during development and aging. Prjna732987. https://www.ncbi.nlm.nih.gov/bioproject/PRJNA732987. Accessed 27 May 2021.